Commun. Comput. Phys.
doi: 10.4208/cicp.040913.220115a

Vol. **18**, No. 2, pp. 450-468
August 2015

On Initial Conditions for the Lattice Boltzmann Method

Juntao Huang[1], Hao Wu[2,*] and Wen-An Yong[1]

[1] *Zhou Pei-Yuan Center for Applied Mathematics, Tsinghua University, Beijing 100084, China.*
[2] *Department of Mathematical Sciences, Tsinghua University, Beijing 100084, China.*

Received 4 September 2013; Accepted (in revised version) 22 January 2015

Abstract. In this paper, we propose two initialization techniques for the lattice Boltzmann method. The first one is based on the theory of asymptotic analysis developed in [M. Junk and W.-A. Yong, Asymptotic Anal., 35(2003)]. By selecting consistent macroscopic quantities, this initialization leads to the second-order convergence for both velocity and pressure. Another one is an improvement of the consistent initial conditions proposed in [R. W. Mei, L.-S. Luo, P. Lallemand and D. d'Humières, Comput. Fluids, 35(2006)]. The improvement involves a modification of the collision term and a reconstruction step. Numerical examples confirm the accuracy and efficiency of our techniques.

AMS subject classifications: 65M06, 76M20

Key words: Lattice Boltzmann method, initial conditions, asymptotic analysis, incompressible Navier-Stokes equation.

1 Introduction

In the past two decades, the lattice Boltzmann method (LBM) [3, 4, 7, 11–13, 19, 26, 27] has emerged as a powerful tool for simulating various fluid flow problems. Because of its simplicity, effectiveness and massive parallelism, the method has been widely used in many flow simulations including thermal flows [9, 10, 21, 25], multi-phase and multi-component flows [22, 28], porous media flows [5, 24], *etc*.

In the meantime, the theoretical study of the LBM has been greatly developed. In the early literature, the macroscopic fluid dynamic equations were obtained from the LBM by using the multi-scale technique [19, 26]. Later, the LBM was regarded as a special discretization of the continuous Boltzmann equation [12, 13]. Furthermore, some important properties (*e.g.* stability conditions, dispersion effects) of the LBM were studied [20].

*Corresponding author. *Email addresses:* huangjt13@mails.tsinghua.edu.cn (J. Huang), hwu@tsinghua.edu.cn (H. Wu), wayong@tsinghua.edu.cn (W.-A. Yong)

 ©2015 Global-Science Press

https://doi.org/10.4208/cicp.040913.220115a Published online by Cambridge University Press

After that, the non-existence of H theorems was proved for some lattice Boltzmann models [32,33]. Recently, a theory of asymptotic analysis, including stability and convergence, for the method were established in a mathematically rigorous fashion [1, 15–18, 30, 34].

Initial conditions are indispensable parts of the LBM. For practical applications, available initial data are only those of macroscopic quantities, *e.g.* density, velocity and temperature, instead of the distribution functions $f_i(t,x)$ in the LBM. A conventional way is to specify the initial distributions $f_i(0,x)$ as equilibrium ones $f_i^{eq}(\rho_0,u_0)$ with (ρ_0,u_0) the initial data of density and velocity. But this seems not correct for flows with strong nonlinearity [35] and can lead to initial layers and thereby poor numerical resolutions. Because of this, a non-equilibrium correction method based on the Chapman-Enskog expansion was proposed [6, 29] to improve the initialization. As pointed out in [23], such methods are cumbersome and not easy to implement in practice since it involves high-order time and spatial derivatives. Another drawback of the previous methods is that the initial density field ρ_0 is required but often not available. To overcome this difficulty, an iterative initialization procedure was proposed in [2, 23] to generate consistent initial conditions. This idea is very effective. However, the pressure is only of first-order accuracy, which seems to be the maximal accuracy for problems with general non-periodic boundary conditions in the literature. We also remark that Van Leemput et al. developed an alternative approach to generate initial conditions for LBM [31].

In this work, we propose two kinds of initializations for the LBM. The first one is obtained by using the theory of asymptotic analysis developed in [16–18] for the LBM. Since high-order corrections are involved, the initial layers can be avoided. Here no time derivatives is involved, quite different from the non-equilibrium correction method [29], so it is easy for implementation. Moreover, the velocity and pressure converge at second order since the macroscopic quantities are chosen in a consistent way. The other one is an improvement of the consistent initial conditions proposed in [23]. It significantly decrease the iteration steps and numerical errors by modifying the collision term and adding an extra reconstruction step. Numerical results show that the new initialization routines significantly improve the existing methods.

The paper is organized as follows. In Section 2, after a brief review on the LBM and its asymptotic analysis theory, we present the high order initial conditions for the LBM. Motivated by the asymptotic analysis, we propose an improvement of the consistent initial conditions in Section 3. In Section 4, numerical examples are provided to show the performance of our methods. Some conclusive remarks are made in Section 5.

2 LBM and its asymptotic analysis

2.1 The lattice Boltzmann method

The general form of the LBM is

$$f_i(t+h^2,x+c_ih)=f_i(t,x)+J_i(\vec{f}(t,x))+\widehat{F}_i,\qquad i=1,2,\cdots,N. \tag{2.1}$$

https://doi.org/10.4208/cicp.040913.220115a Published online by Cambridge University Press

Here $f_i = f_i(t,x)$ is the i-th distribution function, $\widehat{F}_i$ denote the external forcing term, $t \geq 0$, $x \in \mathbb{R}^d$, $h > 0$ is a dimensionless spatial mesh-size, and $\vec{f} := (f_1, f_2, \cdots, f_N)^T$. The discrete velocities c_i and the collision terms $J_i(\vec{f})$ satisfy the following symmetry and conservation relations

$$\{c_1, c_2, \cdots, c_N\} = \{-c_1, -c_2, \cdots, -c_N\}, \tag{2.2a}$$

$$\sum_{i=1}^{N} J_i(\vec{f}) = 0, \quad \sum_{i=1}^{N} c_i J_i(\vec{f}) = 0. \tag{2.2b}$$

In view of the symmetry, for $i \in \{1,2,\cdots,N\}$ we define $\bar{\imath} \in \{1,2,\cdots,N\}$ so that

$$c_{\bar{\imath}} = -c_i. \tag{2.3}$$

Remark 2.1. It is known, see e.g. [15,17,30], that Eq. (2.1) is a special discretization of the discrete-velocity Boltzmann equation with diffusive scaling

$$\partial_t f_i + \frac{1}{h} c_i \cdot \nabla f_i = \frac{1}{h^2} \left(J_i(\vec{f}) + \widehat{F}_i \right).$$

A classical example is the D2Q9 model [26], which will used throughout this paper. It has the following parameters

$$\begin{aligned}
&d = 2, \quad N = 9, \quad c_9 = (0,0)^T, \\
&\{c_1, c_2, c_3, c_4\} = \{(\pm 1, 0)^T, (0, \pm 1)^T\}, \\
&\{c_5, c_6, c_7, c_8\} = \{(\pm 1, \pm 1)^T\}, \\
&J_i(\vec{f}) = \frac{1}{\tau}(f_i^{eq}(\rho, u) - f_i).
\end{aligned}$$

Here τ is a relaxation time, the equilibrium distribution f_i^{eq} can be split into linear and quadratic parts

$$f_i^{eq}(\rho, u) = f_{i,L}(\rho, u) + f_{i,Q}(u, u) \tag{2.4}$$

with

$$\begin{aligned}
&f_{i,L}(\rho, u) = f_i^*(\rho + 3u \cdot c_i), \\
&f_{i,Q}(u, w) = f_i^* \left(\frac{9}{2}(u \cdot c_i)(w \cdot c_i) - \frac{3}{2} u \cdot w \right), \\
&f_i^* = \begin{cases} 4/9, & i = 9, \\ 1/9, & i = 1,2,3,4, \\ 1/36, & i = 5,6,7,8, \end{cases}
\end{aligned}$$

and the quantities ρ and u are determined in terms of the distributions:

$$\rho(t,x) := \sum_{i=1}^{9} f_i, \qquad u(t,x) := \sum_{i=1}^{9} c_i f_i.$$

https://doi.org/10.4208/cicp.040913.220115a Published online by Cambridge University Press

At last, the external forcing term is

$$\widehat{F}_i = F_i h^3, \quad F_i = 3 f_i^* c_i \cdot F,$$

in which $F = (F_x, F_y)^T$ is the external force field, see e.g. [8].

2.2 Asymptotic expansion

Observe that the LBM solutions for (2.1) depend on the small mesh-size h. To investigate the asymptotic behavior as h goes to zero, we follow [17] and seek the Ansatz

$$f_i \sim f_i^{(0)} + \sum_{k=1}^{\infty} h^k f_i^{(k)} \tag{2.5}$$

with $f_i^{(0)} = f_i^*$. This is the Strang expansion in numerical analysis. With this Ansatz, we define

$$\rho^{(k)} = \sum_{i=1}^{9} f_i^{(k)}, \quad u^{(k)} = \sum_{i=1}^{9} c_i f_i^{(k)}$$

for $k = 1,2,\cdots$. It is easy to see that

$$\rho^{(0)} = 1, \quad u^{(0)} = 0.$$

and

$$\rho \sim \rho^{(0)} + \sum_{k=1}^{\infty} h^k \rho^{(k)}, \tag{2.6}$$

$$u \sim u^{(0)} + \sum_{k=1}^{\infty} h^k u^{(k)}. \tag{2.7}$$

Substituting the Ansatz (2.5) into the LBM (2.1) and making use of the Taylor expansion, we have

$$\begin{aligned} &\sum_{k=0}^{\infty} h^k \sum_{s=0}^{k} D_{i,s} f_i^{(k-s)} \\ &= \sum_{k=0}^{\infty} h^k f_i^{(k)} + \frac{1}{\tau} \sum_{k=0}^{\infty} h^k \left(f_{i,L}(\rho^{(k)}, u^{(k)}) + \sum_{s=0}^{k} f_{i,Q}(u^{(s)}, u^{(k-s)}) - f_i^{(k)} \right) + h^3 F_i. \end{aligned} \tag{2.8}$$

Here the differential operator $D_{i,s}$ is defined as

$$D_{i,s} = \sum_{2p+q=s} \frac{\partial_t^p (c_i \cdot \nabla)^q}{p! q!}.$$

https://doi.org/10.4208/cicp.040913.220115a Published online by Cambridge University Press

Notice that $D_{i,0}=1$, $u^{(0)}=0$,$\rho^{(0)}=1$ and $f_i^{(0)}$ is constant. We match the coefficients of h^k in (2.8) to get

$$f_{i,L}(\rho^{(0)},u^{(0)})-f_i^{(0)}=0, \tag{2.9}$$

$$f_{i,L}(\rho^{(1)},u^{(1)})-f_i^{(1)}=0, \tag{2.10}$$

$$\begin{aligned} &D_{i,k-1}f_i^{(1)}+D_{i,k-2}f_i^{(2)}+\cdots+D_{i,1}f_i^{(k-1)}\\ &\quad=\frac{1}{\tau}\left(f_{i,L}(\rho^{(k)},u^{(k)})+\sum_{s=1}^{k-1}f_{i,Q}(u^{(s)},u^{(k-s)})-f_i^{(k)}\right)+\delta_{k3}F_i, \end{aligned} \tag{2.11}$$

for $k\geq 2$. Eq. (2.9) is obvious for $f_{i,L}(1,0)=f_i^*$. From (2.10) it follows that

$$f_i^{(1)}=f_{i,L}(\rho^{(1)},u^{(1)})=f_i^*(\rho^{(1)}+3u^{(1)}\cdot c_i). \tag{2.12}$$

Moreover, from (2.11) we have

$$\begin{aligned} f_i^{(k)}=&f_{i,L}(\rho^{(k)},u^{(k)})+\sum_{s=1}^{k-1}f_{i,Q}(u^{(s)},u^{(k-s)})\\ &-\tau\left(D_{i,k-1}f_i^{(1)}+D_{i,k-2}f_i^{(2)}+\cdots+D_{i,1}f_i^{(k-1)}\right)+\tau\delta_{k3}F_i. \end{aligned} \tag{2.13}$$

This means that $f_i^{(k)}$ can be inductively determined by $\rho^{(s)},u^{(s)}\,(1\leq s\leq k)$ and their derivatives. Note that $\rho^{(k)}$ and $u^{(k)}$ are determined by $f_i^{(k)}$.

In order to determine $f_i^{(k)}$ completely, we slightly modify the proof of Lemma 3.1 in [17] to get the following theorem.

Theorem 2.1. *For $k=0,1,2\cdots$, assume $\rho^{(2k+1)}(0,x)=0$, $u^{(2k)}(0,x)=0$ and periodic boundary conditions are posed. Then the expansion coefficients satisfy*

$$\begin{aligned} &f_i^{(2k)}=f_{\bar{i}}^{(2k)},\quad f_i^{(2k+1)}=-f_{\bar{i}}^{(2k+1)},\\ &\rho^{(2k+1)}(t,x)=0,\quad u^{(2k)}(t,x)=0. \end{aligned}$$

The coefficients $\rho^{(2)}$ and $u^{(1)}$ solve the incompressible Navier-Stokes equations

$$\partial_t u^{(1)}+u^{(1)}\cdot\nabla u^{(1)}+\frac{1}{3}\nabla\rho^{(2)}=\nu\triangle u^{(1)}+F, \tag{2.14}$$

$$\nabla\cdot u^{(1)}=0, \tag{2.15}$$

with the viscosity coefficient $\nu=\frac{1}{3}(\tau-\frac{1}{2})$. Furthermore, the coefficients $\rho^{(2k)}$ and $u^{(2k+1)}$ with $k\geq 1$ satisfy the following linear equations

$$\begin{aligned} &\partial_t u^{(2k+1)}+u^{(1)}\cdot\nabla u^{(2k+1)}+u^{(2k+1)}\cdot\nabla u^{(1)}+\frac{1}{3}\nabla\rho^{(2k+2)}=\nu\triangle u^{(2k+1)}+G_1^{(2k+1)},\\ &\nabla\cdot u^{(2k+1)}=-\partial_t\rho^{(2k)}+G_2^{(2k+1)} \end{aligned}$$

https://doi.org/10.4208/cicp.040913.220115a Published online by Cambridge University Press

with the source term $G_1^{(2k+1)}$ *and* $G_2^{(2k+1)}$ *depending only on derivatives of* $F, \rho^{(\ell)}$ *and* $u^{(\ell)}$ *with* $\ell < 2k+1$.

As a corollary of the last theorem, the asymptotic expansions in (2.6) and (2.7) are reduced to

$$\begin{aligned}\rho &\sim 1+h^2\rho^{(2)}+h^4\rho^{(4)}+\cdots,\\ u &\sim hu^{(1)}+h^3u^{(3)}+\cdots.\end{aligned}$$

Thus, the solution (p,v) of the incompressible Navier-Stokes equations is given by

$$p=\frac{1}{3}\rho^{(2)}=\frac{1}{3h^2}\left(\sum_{i=1}^{9}f_i-1\right)+\mathcal{O}(h^2), \tag{2.16}$$

$$v=u^{(1)}=\frac{1}{h}\sum_{i=1}^{9}c_if_i+\mathcal{O}(h^2). \tag{2.17}$$

2.3 Initial conditions for the LBM

As a result of Theorem 2.1 and Eq. (2.12), the first-order expansion coefficient is given by

$$f_i^{(1)}=3f_i^*u^{(1)}\cdot c_i. \tag{2.18}$$

Plugging this into (2.13) with $k=2$ leads to

$$\begin{aligned}f_i^{(2)}&=f_{i,L}(\rho^{(2)},u^{(2)})+f_{i,Q}(u^{(1)},u^{(1)})-\tau(c_i\cdot\nabla)f_i^{(1)}\\ &=f_i^*\rho^{(2)}+f_{i,Q}(u^{(1)},u^{(1)})-3\tau f_i^*c_i\cdot\nabla(u^{(1)}\cdot c_i).\end{aligned} \tag{2.19}$$

Furthermore, $f_i^{(3)}$ has the following expression

$$\begin{aligned}f_i^{(3)}&=f_{i,L}(\rho^{(3)},u^{(3)})-\tau\left(\partial_tf_i^{(1)}+\frac{1}{2}(c_i\cdot\nabla)^2f_i^{(1)}+c_i\cdot\nabla f_i^{(2)}\right)+\tau F_i\\ &=3f_i^*u^{(3)}\cdot c_i-3\tau f_i^*\partial_tu^{(1)}\cdot c_i-\frac{3}{2}\tau f_i^*(c_i\cdot\nabla)^2(u^{(1)}\cdot c_i)+\tau F_i\\ &\quad-\tau c_i\cdot\nabla\left(f_i^*\rho^{(2)}+f_{i,Q}(u^{(1)},u^{(1)})-3\tau f_i^*c_i\cdot\nabla(u^{(1)}\cdot c_i)\right)\\ &=3f_i^*u^{(3)}\cdot c_i+3\tau f_i^*c_i\cdot(u^{(1)}\cdot\nabla u^{(1)}-\nu\triangle u^{(1)})\\ &\quad-\tau c_i\cdot\nabla f_{i,Q}(u^{(1)},u^{(1)})+3\tau\left(\tau-\frac{1}{2}\right)f_i^*(c_i\cdot\nabla)^2(u^{(1)}\cdot c_i).\end{aligned} \tag{2.20}$$

In the above derivation, the incompressible Navier-Stokes equations (2.14) are used to replace the time derivative $\partial_tu^{(1)}$. According to (2.5) and (2.18)-(2.20), we can write the

https://doi.org/10.4208/cicp.040913.220115a Published online by Cambridge University Press

distribution function as

$$\begin{aligned} f_i &= f_i^{(0)} + h f_i^{(1)} + h^2 f_i^{(2)} + h^3 f_i^{(3)} + \mathcal{O}(h^4) \\ &= f_i^{eq}(1, hu^{(1)}) - h\tau c_i \cdot \nabla f_i^{eq}(0, hu^{(1)}) + h^2 f_i^* \rho^{(2)} \\ &\quad + 3h^3 f_i^* u^{(3)} \cdot c_i + 3h^3 \tau f_i^* c_i \cdot (u^{(1)} \cdot \nabla u^{(1)} - \nu \triangle u^{(1)}) \\ &\quad + 3h^3 \tau \Big(\tau - \frac{1}{2}\Big) f_i^* (c_i \cdot \nabla)^2 (u^{(1)} \cdot c_i) + \mathcal{O}(h^4). \end{aligned} \tag{2.21}$$

In view of the consistency of macroscopic quantities

$$\rho^{(2)}(0,x) = 3p_0(x), \quad u^{(1)}(0,x) = v_0(x),$$

we take the initial distributions as

$$\begin{aligned} f_i(0,x) &= f_i^{eq}(1, hv_0) - h\tau c_i \cdot \nabla f_i^{eq}(0, hv_0) + 3h^2 f_i^* p_0 \\ &\quad + 3h^3 \tau f_i^* \left(c_i \cdot (v_0 \cdot \nabla v_0 - \nu \triangle v_0) + \Big(\tau - \frac{1}{2}\Big)(c_i \cdot \nabla)^2 (v_0 \cdot c_i) \right) + 3h^3 f_i^* u^{(3)}(0,x) \cdot c_i. \end{aligned} \tag{2.22}$$

It remains to choose $u^{(3)}(0,x)$. To this end, we recall from Theorem 2.1 that

$$\nabla \cdot u^{(3)}(0,x) = -\partial_t \rho^{(2)}(0,x) - \frac{1}{2} \nabla \cdot F, \tag{2.23}$$

Remark that the time derivative is involved here and there are infinitely many $u^{(3)}(0,x)$ satisfying Eq. (2.23). For definiteness, we suggest to take $\widetilde{u}^{(3)}(0,x) = u^{(3)}(0,x) + \frac{1}{2}F$ solving the following Poisson equation

$$\begin{aligned} \frac{1}{3} \triangle \widetilde{u}^{(3)}(0,x) &= \nu(\triangle v_0 \cdot \nabla v_0 + v_0 \cdot \nabla(\triangle v_0)) \\ &\quad - \big(\nabla p_0 \cdot \nabla v_0 + v_0 \cdot \nabla^2 p_0\big) \\ &\quad - ((v_0 \cdot \nabla v_0) \cdot \nabla v_0 + v_0 \cdot \nabla (v_0 \cdot \nabla v_0)). \end{aligned} \tag{2.24}$$

The reason is given in the appendix.

As shown in [16], the above choice of initial distributions ensures that the LB solutions have the following asymptotic expansion

$$f_i(t,x) = f_i^{(0)} + h f_i^{(1)} + h^2 f_i^{(2)} + h^3 f_i^{(3)} + \mathcal{O}(h^4)$$

in the usual L^2-norm. Referring to (2.16) and (2.17), we have second-order convergence for both the velocity and pressure.

Remark 2.2. We can also take the following

$$f_i(0,x) = f_i^{eq}(1, hv_0) + 3h^2 f_i^* (p_0 - \tau c_i \cdot \nabla (v_0 \cdot c_i)). \tag{2.25}$$

https://doi.org/10.4208/cicp.040913.220115a Published online by Cambridge University Press

as initial distributions. This formula is simpler than that in (2.22). But it only ensures the following asymptotic expansion

$$f_i(t,x)=f_i^{(0)}+hf_i^{(1)}+h^2f_i^{(2)}+\mathcal{O}(h^3).$$

Referring to (2.16) and (2.17), we have only first-order convergence for the pressure, while second-order convergence for the velocity.

3 An improvement of the consistent initial conditions

In [23], a simple and effective iteration method was proposed to generate consistent initial conditions when the initial pressure $p_0(x)$ is not known. The key idea can be expressed with the following LBM-like scheme

$$f_i(t+h^2,x+c_ih)=f_i(t,x)+J_i^{old}(\vec{f}(t,x))+\widehat{F}_i,\quad 1=1,2,\cdots,N. \tag{3.1}$$

Here the collision term is given by

$$J_i^{old}(\vec{f})=\frac{1}{\tau}\left(f_i^{eq}(\rho,hv_0)-f_i\right), \tag{3.2}$$

and v_0 is the initial velocity field. Multiplying the collision term by c_i and summing over index i leads to

$$\sum_i c_iJ_i^{old}(\vec{f})=\frac{hv_0-u}{\tau}\neq 0$$

in general. This means that $u:=\sum_i c_if_i$ is not a collision invariant, in contrast with (2.2).

To fix this problem, we refer to the decomposition in (2.4) and propose the following new collision

$$J_i^{new}(\vec{f})=\frac{1}{\tau}\left(f_{i,L}(\rho,u)+f_{i,Q}(hv_0,hv_0)-f_i\right). \tag{3.3}$$

A simple calculation shows that

$$\sum_i J_i^{new}(\vec{f})=0,\quad \sum_i c_iJ_i^{new}(\vec{f})=0.$$

Substituting the Ansatz (2.5) into (3.1) with the new collision term (3.3) and making use of the Taylor expansion, we have

$$\begin{aligned}&\sum_{k=0}^{\infty}h^k\sum_{s=0}^{k}D_{i,s}f_i^{(k-s)}\\&=\sum_{k=0}^{\infty}h^kf_i^{(k)}+\frac{1}{\tau}\sum_{k=0}^{\infty}h^k\left(f_{i,L}(\rho^{(k)},u^{(k)})+f_{i,Q}(v_0,v_0)\delta_{k2}-f_i^{(k)}\right)\end{aligned} \tag{3.4}$$

https://doi.org/10.4208/cicp.040913.220115a Published online by Cambridge University Press

with $\delta_{k2}=1$ if $k=2$ and otherwise $\delta_{k2}=0$. Matching the coefficients of h^k in (3.4), we obtain

$$0=f_{i,L}(\rho^{(0)},u^{(0)})-f_i^{(0)}, \tag{3.5}$$

$$0=f_{i,L}(\rho^{(1)},u^{(1)})-f_i^{(1)}, \tag{3.6}$$

$$c_i\cdot\nabla f_i^{(1)}=\frac{1}{\tau}\left(f_{i,L}(\rho^{(2)},u^{(2)})+f_{i,Q}(v_0,v_0)-f_i^{(2)}\right), \tag{3.7}$$

$$\begin{aligned}&D_{i,k-1}f_i^{(1)}+D_{i,k-2}f_i^{(2)}+\cdots+D_{i,1}f_i^{(k-1)}\\&\quad=\frac{1}{\tau}\left(f_{i,L}(\rho^{(k)},u^{(k)})-f_i^{(k)}\right)+\delta_{k3}F_i\end{aligned} \tag{3.8}$$

for $k\geq 3$.

As in the previous section, (3.5) is obviously true. Multiplying (3.7) by 1 and c_i and then summing the resultant relations over index i we obtain

$$\nabla\cdot u^{(1)}=0, \tag{3.9}$$

$$\nabla\rho^{(1)}=0. \tag{3.10}$$

Next, we integrate (3.8) with $k=3$ over the computational domain Ω and sum over index i to get

$$\partial_t\left(\int_\Omega\rho^{(1)}\mathrm{d}x\right)=0,$$

where the periodic boundary condition for $f^{(k)}$ are used. This, together with (3.10) and the initial condition $\rho^{(1)}(0,x)=0$, leads to

$$\rho^{(1)}(t,x)=0,\quad \forall t>0. \tag{3.11}$$

Thus, (2.18) still holds: $f_i^{(1)}=3f_i^*u^{(1)}\cdot c_i$. Moreover, Eq. (3.7) can be rewritten as

$$f_i^{(2)}=f_{i,L}(\rho^{(2)},u^{(2)})+f_{i,Q}(v_0,v_0)-\tau c_i\cdot\nabla f_i^{(1)}. \tag{3.12}$$

Now we multiply (3.8) with $k=3$ by c_i, sum the resultant relation over index i and use (3.12) to obtain

$$\partial_t u^{(1)}+v_0\cdot\nabla v_0+\frac{1}{3}\nabla\rho^{(2)}=\nu\triangle u^{(1)}+F. \tag{3.13}$$

With the divergence operator acting on the two sides of the last equation and using (3.9), we see that the pressure $p_0=\frac{1}{3}\rho^{(2)}$ is consistent to the initial velocity field

$$\nabla\cdot(v_0\cdot\nabla v_0)+\triangle p_0=\nabla\cdot F.$$

On the other hand, Eq. (3.13) together with (3.9) constitutes the non-homogeneous Stokes equations with v_0 given. The Taylor-Green flow in Section 4 shows that these

https://doi.org/10.4208/cicp.040913.220115a Published online by Cambridge University Press

equations could have a solution $u^{(1)} \neq v_0$. Therefore the distribution functions f_i cannot provide reasonable initial conditions with the new collision term (3.3).

To fix this problem, we propose the follow algorithm with a reset step. The distribution functions f_i are reconstructed by using the formula (2.25) with initial pressure p_0 as follows.

(1) For $k=0$, take the initial distribution function $f_i^{*,k}(x)$ by using the formula (2.25) with $p_0^k=0$.

(2) Execute the LBM

$$\tilde{f}_i^{k+1}(x+c_ih) = f_i^{*,k}(x) + \frac{1}{\tau}\left(f_{i,L}(\rho^{*,k},u^{*,k}) + f_{i,Q}(hv_0,hv_0) - f_i^{*,k}(x)\right) + \widehat{F}_i,$$

where $\rho^{*,k}$ and $u^{*,k}$ is determined by

$$\rho^{*,k} = \sum_{i=1}^{9} f_i^{*,k}, \quad u^{*,k} = \sum_{i=1}^{9} c_i f_i^{*,k}.$$

(3) Compute p_0^{k+1} with the formula

$$p_0^{k+1} = \frac{1}{3h^2}\left(\sum_{i=1}^{9} \tilde{f}_i^{k+1} - 1\right).$$

Then compute $f_i^{*,k+1}(x)$ with formula (2.25) with p_0^{k+1}. If $\left\|p_0^k - p_0^{k+1}\right\|_2$ is small enough, namely, the pressure p_0 converges, then output $f_i^{*,k+1}(x)$ and stop.

(4) Otherwise, set $k=k+1$ and repeat the steps (2)-(4).

The output of this algorithm will be our initial distributions for the LBM:

$$f_i(0,x) = f_i^{*,k+1}(x) \tag{3.14}$$

with k the total iteration steps.

Remark 3.1. To see our algorithm more clearly, let us rewrite it in a compact form by eliminating $f_i^{*,k}$. For this purpose, we compute $\rho^{*,k}$ by using (2.25) to obtain

$$\begin{aligned}\rho^{*,k} &= \sum_{i=1}^{9} f_i^{*,k} = 1 + 3h^2 p_0^k - 3h^2\tau \sum_{i=1}^{9} (f_i^* c_i \cdot \nabla(v_0 \cdot c_i)) \\ &= 1 + 3h^2 p_0^k - h^2\tau \nabla \cdot v_0 \\ &= 1 + 3h^2 p_0^k.\end{aligned}$$

https://doi.org/10.4208/cicp.040913.220115a Published online by Cambridge University Press

In the last step we have used the fact that the divergence of v_0 equals to zero. Substituting the expressions of $\rho^{*,k}$ and $f_i^{*,k}$ into the evolution equation in step (2), we arrive at

$$\tilde{f}_i^{k+1}(x+c_ih)=f_i^{eq}(\tilde{\rho}^k(x),hv_0(x))-3h^2f_i^*(\tau-1)c_i\cdot\nabla(v_0(x)\cdot c_i)+\widehat{F}_i, \tag{3.15}$$

where $\tilde{\rho}^k$ is given with

$$\tilde{\rho}^k=\sum_{i=1}^{9}\tilde{f}_i^k.$$

In conclusion, our algorithm can be presented in a more concise form:

(1) For $k=0$, we take

$$\tilde{f}_i^0(x)=f_i^{eq}(1,hv_0(x-c_ih))-3h^2f_i^*(\tau-1)c_i\cdot\nabla(v_0(x-c_ih)\cdot c_i)+\widehat{F}_i.$$

(2) For $k\geq 0$, execute the iteration

$$\tilde{f}_i^{k+1}(x+c_ih)=f_i^{eq}(\tilde{\rho}^k(x),hv_0(x))-3h^2f_i^*(\tau-1)c_i\cdot\nabla(v_0(x)\cdot c_i)+\widehat{F}_i,$$

where $\tilde{\rho}^k$ is given by

$$\tilde{\rho}^k=\sum_{i=1}^{9}\tilde{f}_i^k.$$

(3) Compute p_0^{k+1} with the formula

$$p_0^{k+1}=\frac{1}{3h^2}\left(\sum_{i=1}^{9}\tilde{f}_i^{k+1}-1\right).$$

(4) If $\|p_0^k-p_0^{k+1}\|_2$ is small enough, then take the formula (2.25) with p_0^{k+1} as our initial distributions for the LBM. Otherwise, set $k=k+1$ and go to step (2).

4 Numerical examples

In this section, we test the accuracy and efficiency of our initialization techniques by several numerical examples. The incompressible Navier-Stokes equations (2.14)-(2.15) are simulated in the periodic domain $\Omega=[0,1]^2$. The mesh size $\Delta x=\Delta y=h$ and the time step $\Delta t=h^2$ are set according to the preceding analysis. Let $N=1/h$ be the number of grids in each spatial direction.

Apart from the velocity and pressure, the normalized total kinetic energy and the normalized projection of the pressure will also be computed:

$$K(t)=\frac{2}{N^2U_0^2}\iint_\Omega(u_x^2+u_y^2)\,\mathrm{d}x\mathrm{d}y,$$

$$P_2(t)=-\frac{16}{N^2U_0^2}\iint_\Omega p(t,x,y)\cos(2\pi(x+y))\cos(2\pi(x-y))\,\mathrm{d}x\mathrm{d}y.$$

https://doi.org/10.4208/cicp.040913.220115a Published online by Cambridge University Press

Here $U_0=0.05$ is the initial velocity amplitude, which will be used later. The relaxation time τ is taken as 0.506 or 0.65, to which the corresponding viscosity $\nu=\frac{1}{3}(\tau-\frac{1}{2})$ is 0.002 or 0.05. And we define the numerical errors as follows

$$
\begin{aligned}
e_u(T)&=\sup_{t\in[0,T]}\left(\iint_\Omega|u^{\rm num}(t)-u^{\rm exa}(t)|^2{\rm d}x{\rm d}y\right)^{1/2},\\
e_p(T)&=\sup_{t\in[0,T]}\left(\iint_\Omega|p^{\rm num}(t)-p^{\rm exa}(t)|^2{\rm d}x{\rm d}y\right)^{1/2},\\
e_K(T)&=\sup_{t\in[0,T]}|K^{\rm num}(t)-K^{\rm exa}(t)|,\\
e_{P_2}(T)&=\sup_{t\in[0,T]}|P_2^{\rm num}(t)-P_2^{\rm exa}(t)|.
\end{aligned}
$$

4.1 The Taylor-Green vortex flow

We firstly consider the Taylor-Green vortex flow, see e.g. [23]. The external force field $F=(0,0)^T$, and the analytic solution is given by

$$u_x(t,x,y)=-U_0\cos(2\pi x)\sin(2\pi y)e^{-8\pi^2\nu t}, \tag{4.1}$$

$$u_y(t,x,y)=U_0\cos(2\pi y)\sin(2\pi x)e^{-8\pi^2\nu t}, \tag{4.2}$$

$$p(t,x,y)=-\frac{1}{2}U_0^2\cos(2\pi(x+y))\cos(2\pi(x-y))e^{-16\pi^2\nu t}. \tag{4.3}$$

Example 4.1. In this example, we test the numerical errors of LBM. The initial distributions $f_i(0,x)$ are given by (2.22). According to (4.1)-(4.3), $v_0(x,y)$ and $p_0(x,y)$ can be given explicitly for (2.22) as

$$
\begin{aligned}
v_0(x,y)&=U_0(-\cos(2\pi x)\sin(2\pi y),\cos(2\pi y)\sin(2\pi x)),\\
p_0(x,y)&=-\frac{1}{2}U_0^2\cos(2\pi(x+y))\cos(2\pi(x-y)).
\end{aligned}
$$

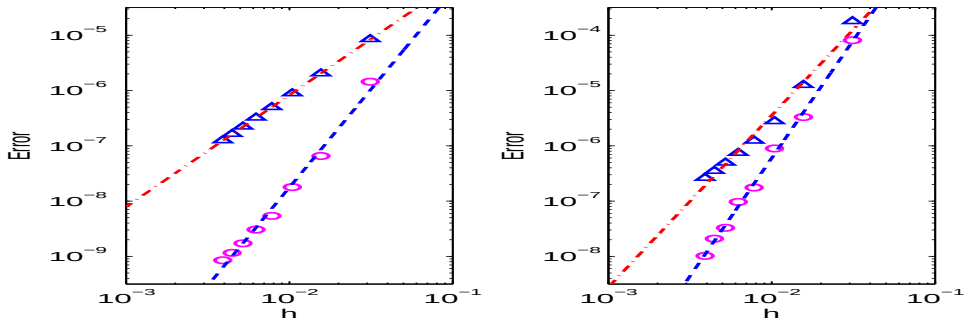
And $u^{(3)}(0,x,y)$ in (2.22) is taken as

$$u^{(3)}(0,x,y)=-6\pi\nu U_0^2(\sin(2\pi x)\cos(2\pi x),\sin(2\pi y)\cos(2\pi y)),$$

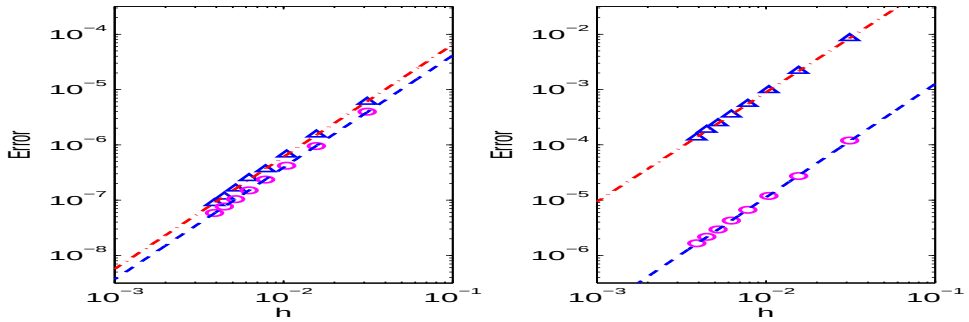
which satisfies the Poisson equation (2.24).

In Fig. 1, the numerical errors with different h are output. The results of data fitting indicate the convergence rate in h in Table 1. From which, we can see the convergence rates are not less than second order.

https://doi.org/10.4208/cicp.040913.220115a Published online by Cambridge University Press



(a) $\nu=0.002$



(b) $\nu=0.05$

Figure 1: Example 4.1: Numerical results for $T=1$. Left: blue triangles denote e_p, pink rings denote e_u, the red dash-dot line and the blue dashed line are their fitting results. Right: blue triangles denote e_{P_2}, pink rings denote e_K, the red dash-dot line and the blue dashed line are their fitting results.

Table 1: Example 4.1: the convergence rate in h for different variables at $T=1$.

ν	$u(t,x,y)$	$p(t,x,y)$	$K(t)$	$P_2(t)$
0.002	3.55	2.02	4.27	3.11
0.05	2.02	2.03	2.05	1.98

Example 4.2. In this example, the new initialization algorithm described in Section 3 is tested. We also make a comparison with Mei et al.'s iteration method [23]. In this example, the initial pressure

$$p_0(x,y)=-\frac{1}{2}U_0^2\cos(2\pi(x+y))\cos(2\pi(x-y))$$

is not *a prior* known. The key idea of the iteration is to obtain the numerical initial pressure $\widetilde{p}_0(x,y)$ based on the initial velocity $v_0(x,y)$. In Figs. 2 and 3, the ℓ^2 errors of the initial pressure $\|p_0-\widetilde{p}_0\|_2$ versus the virtual time t_v are plotted for different h and ν. Since the iteration step K is dependent on the small parameter h, the virtual time $t_v=K\Delta t=Kh^2$

https://doi.org/10.4208/cicp.040913.220115a Published online by Cambridge University Press

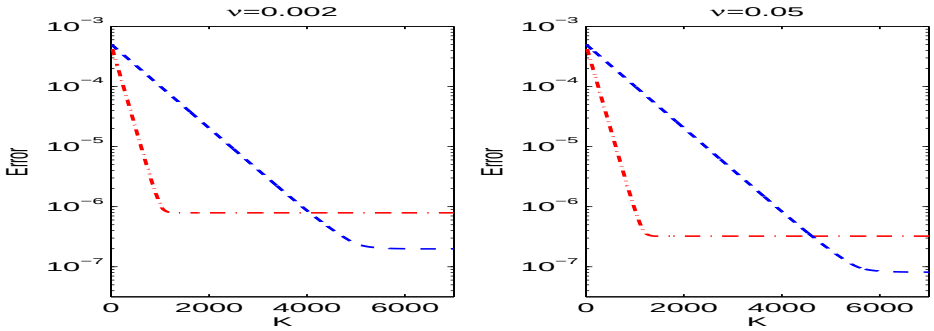


Figure 2: Example 4.2: the ℓ^2 errors of the initial pressure $\|p_0-\widetilde{p}_0\|_2$ versus the number of iterations K. The red dash-dot line and the blue dashed line corresponding to $h=\frac{1}{64}$ and $\frac{1}{128}$ respectively.

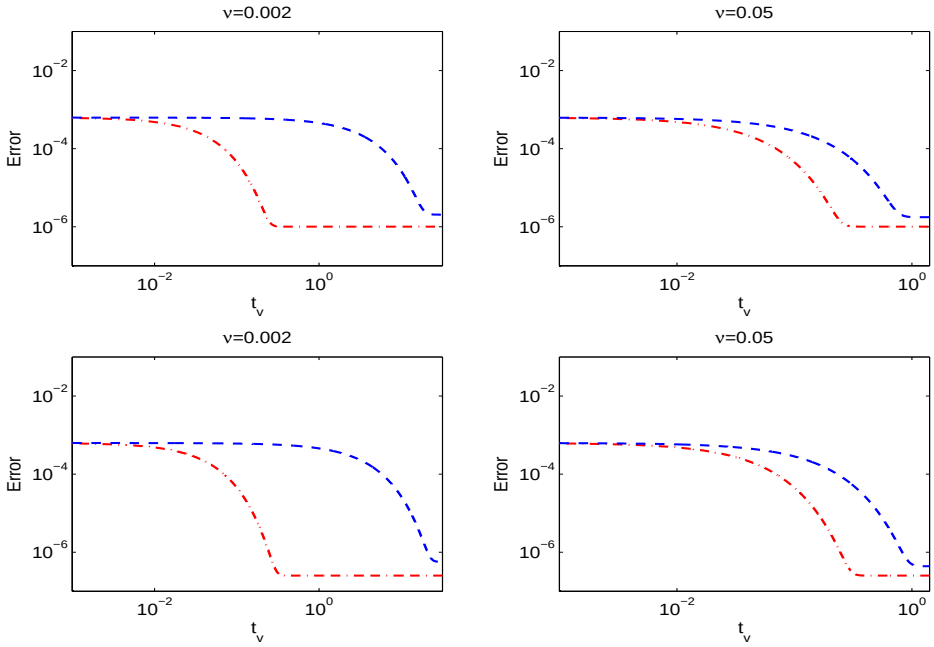


Figure 3: Example 4.2: the ℓ^2 errors of the initial pressure $\|p_0-\widetilde{p}_0\|_2$ versus the virtual time t_v. In each figure, the red dash-dot line is our method and the blue dashed line is Mei et al.'s method. Top: $h=\frac{1}{64}$; Bottom: $h=\frac{1}{128}$.

is introduced to measure the convergence speed. From the figures, we can see that our method converges much faster than Mei et al.'s iteration. Moreover, the virtual time is almost independent of h. We notice that the convergence trend can not last as iteration increasing, since the discretization error would dominate the total error.

https://doi.org/10.4208/cicp.040913.220115a Published online by Cambridge University Press

4.2 The flow with external force field

Consider the following analytic solution for the incompressible Navier-Stokes equations

$$u_x(t,x,y) = U_0(-2\pi U_0 t e^{-4\pi^2\nu t}\cos(2\pi y) + e^{-2\pi^2\nu t}\sin(2\pi y)), \tag{4.4}$$

$$u_y(t,x,y) = U_0 e^{-2\pi^2\nu t}, \tag{4.5}$$

$$p(t,x,y) = \pi\nu U_0 e^{-2\pi^2\nu t}\cos(2\pi y). \tag{4.6}$$

The external force field is as follows

$$F_x = U_0(2\pi^2\nu e^{-2\pi^2\nu t} + 4\pi^2 U_0^2 t e^{-6\pi^2\nu t})\sin(2\pi y),$$
$$F_y = -2U_0\pi^2\nu e^{-2\pi^2 t\nu}(1+\sin(2\pi y)).$$

Example 4.3. We test the numerical errors of the LBM in this example. The distribution function is initialization by (2.22), here $v_0(x,y)$ and $p_0(x,y)$ can be explicitly given according to (4.4)-(4.6) as

$$v_0(x,y) = U_0(\sin(2\pi y),1),$$
$$p_0(x,y) = \pi\nu U_0\cos(2\pi y).$$

And $u^{(3)}(0,x,y)$ is taken as

$$u^{(3)}(0,x,y) = (0,3\pi^2\nu^2 U_0\sin(2\pi y)) - \frac{1}{2}F(0,x,y).$$

which consistent to (2.23).

In Fig. 4, the numerical errors with different h are output. The results of data fitting indicate the convergence rate in h in Table 2. From which, we can draw the same conclusion as in Example 4.1.

Table 2: Example 4.3: the convergence rate in h for different variables at $T=1$.

ν	$u(t,x,y)$	$p(t,x,y)$
0.002	2.01	2.00
0.05	2.00	2.00

Example 4.4. As in Example 4.2, we numerically test the modified iteration initialization. In Figs. 5 and 6, the ℓ^2 errors of the initial pressure $\|p_0-\widetilde{p_0}\|_2$ versus the virtual time t_v are plotted for different h and ν. From the figures, we can see the new algorithm remarkably improves the accuracy.

Remark 4.1. The numerical results have indicated that the initialization iteration will converge before the virtual time $t_v \approx 0.5$. Compared with the total computational cost of the LBM, the additional cost of the initialization algorithm is quite minor.

https://doi.org/10.4208/cicp.040913.220115a Published online by Cambridge University Press

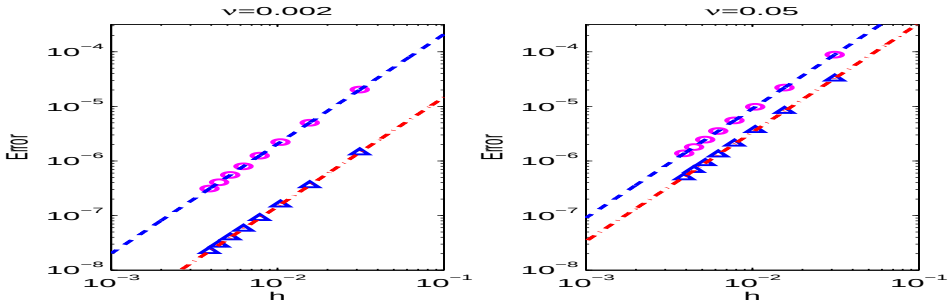


Figure 4: Example 4.3: Numerical results for $T=1$. Blue triangles denote e_p, pink rings denote e_u, the red dash-dot line and the blue dashed line are their fitting results.

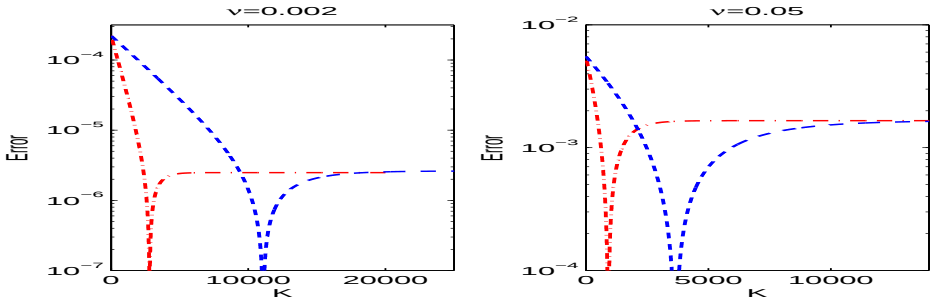


Figure 5: Example 4.4: the ℓ^2 errors of the initial pressure $\|p_0-\widetilde{p}_0\|_2$ versus the number of iterations K. The red dash-dot line and the blue dashed line corresponding to $h=\frac{1}{64}$ and $\frac{1}{128}$ respectively.

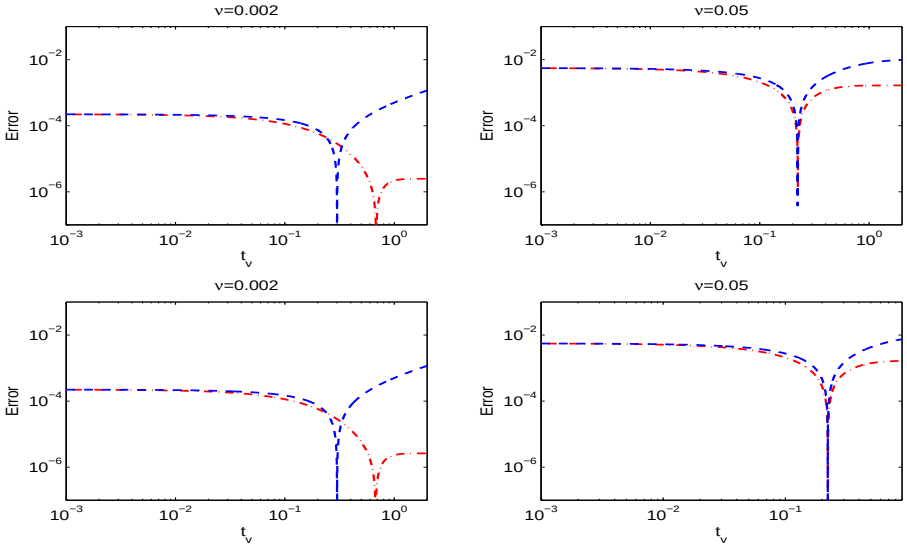


Figure 6: Example 4.4: the ℓ^2 errors of the initial pressure $\|p_0-\widetilde{p}_0\|_2$ versus the virtual time t_v. In each figure, the red dash-dot line is our method and the blue dashed line is Mei et al.'s method. Top: $h=\frac{1}{64}$; Bottom: $h=\frac{1}{128}$.

https://doi.org/10.4208/cicp.040913.220115a Published online by Cambridge University Press

5 Conclusion

Two kinds of initialization for the LBM are proposed based on the theory of asymptotic analysis in the diffusive scaling. By involving high-order corrections and choosing consistent macroscopic quantities, the method can be very accurate. In particular, we suggest an initialization, which ensures the second order convergence rate for the velocity and pressure for the incompressible Navier-Stokes equation. The other approach significantly improves the efficiency and accuracy of the iteration initialization when the initial pressure is not a prior given. The key idea of this approach is to introduce a modification of the collision term and a new reconstruction step. We verify the accuracy and efficiency of the idea by several numerical examples. An interesting question is how to apply these initializations for the LBM with multiple-relaxation-time (MRT). We are currently investigating this important extension and hope to report our progress in the near future [14].

Acknowledgments

The second author would like to thank Prof. L.-S. Luo and Prof. Z.X. Yang for their valuable comments in improving the quality of the manuscript. This work was partially supported by SRF for ROCS, SEM; NSFC project 11101236 and NSFC project 11471185.

Appendix

From Theorem 2.1, we can see

$$\nabla\cdot\widetilde{u}^{(3)}=-\partial_t\rho^{(2)}. \tag{A.1}$$

As we have discussed in Section 2.3, it is not easy to get $\widetilde{u}^{(3)}$ by using (A.1). Thus, we take divergence of (2.14) to obtain

$$\nabla\cdot(u^{(1)}\cdot\nabla u^{(1)})+\frac{1}{3}\triangle\rho^{(2)}=0. \tag{A.2}$$

By comparing with the term $\partial_t(\triangle\rho^{(2)})$, we can get the following equation

$$\triangle\widetilde{u}^{(3)}=3\partial_t(u^{(1)}\cdot\nabla u^{(1)}) \tag{A.3}$$

from (A.1) and (A.2). Eliminating the time derivative in (A.3) by using (2.14) leads to the Poisson equation:

https://doi.org/10.4208/cicp.040913.220115a Published online by Cambridge University Press

$$\begin{aligned}\frac{1}{3}\triangle\widetilde{u}^{(3)} &= (\partial_t u^{(1)})\cdot\nabla u^{(1)} + u^{(1)}\cdot\nabla(\partial_t u^{(1)})\\ &= \Big(\nu\triangle u^{(1)} - u^{(1)}\cdot\nabla u^{(1)} - \frac{1}{3}\nabla\rho^{(2)}\Big)\cdot\nabla u^{(1)} + u^{(1)}\cdot\nabla\Big(\nu\triangle u^{(1)} - u^{(1)}\cdot\nabla u^{(1)} - \frac{1}{3}\nabla\rho^{(2)}\Big)\\ &= \nu\Big(\triangle u^{(1)}\cdot\nabla u^{(1)} + u^{(1)}\cdot\nabla(\triangle u^{(1)})\Big) - \frac{1}{3}\Big(\nabla\rho^{(2)}\cdot\nabla u^{(1)} + u^{(1)}\cdot\nabla^2\rho^{(2)}\Big)\\ &\quad - \Big((u^{(1)}\cdot\nabla u^{(1)})\cdot\nabla u^{(1)} + u^{(1)}\cdot\nabla(u^{(1)}\cdot\nabla u^{(1)})\Big).\end{aligned}$$

References

[1] M.K. Banda, W.-A. Yong, and A. Klar. A stability notion for lattice boltzmann equations. *SIAM Journal on Scientific Computing*, 27:2098–2111, 2006.

[2] A. Caiazzo. Analysis of lattice Boltzmann initialization routines. *Journal of Statistical Physics*, 121:37–48, 2005.

[3] H.D. Chen, S.Y. Chen, and W. Matthaeus. Recovery of the Navier-Stokes equations using a lattice-gas Boltzmann method. *Physical Review A*, 45:5339–5342, 1992.

[4] S.Y. Chen and G.D. Doolen. Lattice Boltzmann method for fluid flows. *Annual Review of Fluid Mechanics*, 30:329–364, 1998.

[5] Z.L. Guo and T.S. Zhao. Lattice Boltzmann model for incompressible flows through porous media. *Physical Review E*, 66:036304, 2002.

[6] Z.L. Guo and T.S. Zhao. Explicit finite-difference lattice Boltzmann method for curvilinear coordinates. *Physical Review E*, 67:066709, 2003.

[7] Z.L. Guo and C.G. Zheng. *Theory and Applications of Lattice Boltzmann Method*. Science Press, Beijing, 2008. in Chinese.

[8] Z.L. Guo, C.G. Zheng, and B.C. Shi. Discrete lattice effects on the forcing term in the lattice Boltzmann method. *Physical Review E*, 65:046308, 2002.

[9] Z.L. Guo, C.G. Zheng, B.C. Shi, and T.S. Zhao. Thermal lattice Boltzmann equation for low Mach number flows: Decoupling model. *Physical Review E*, 75:036704, 2007.

[10] X.Y. He, S.Y. Chen, and G.D. Doolen. A novel thermal model for the lattice Boltzmann method in incompressible limit. *Journal of Computational Physics*, 146:282–300, 1998.

[11] X.Y. He and L.-S. Luo. Lattice Boltzmann model for the incompressible Navier-Stokes equation. *Journal of Statistical Physics*, 88:927–944, 1997.

[12] X.Y. He and L.-S. Luo. A priori derivation of the lattice Boltzmann equation. *Physical Review E*, 55:6333–6336, 1997.

[13] X.Y. He and L.-S. Luo. Theory of the lattice Boltzmann method: From the Boltzmann equation to the lattice Boltzmann equation. *Physical Review E*, 56:6811–6817, 1997.

[14] J.T. Huang, T. Liu, H. Wu, and W.-A. Yong. Numerical analysis and high order initialization of MRT-LBM, 2013. submitted.

[15] T. Inamuro, M. Yoshino, and F. Ogino. Accuracy of the lattice Boltzmann method for small Knudsen number with finite reynolds number. *Phys. Fluids*, 9:3535–3542, 1997.

[16] M. Junk and Z.X. Yang. Convergence of lattice Boltzmann methods for Navier-Stokes flows in periodic and bounded domains. *Numerische Mathematik*, 112:65–87, 2009.

[17] M. Junk and W.-A. Yong. Rigorous Navier-Stokes limit of the lattice Boltzmann equation. *Asymptotic Analysis*, 35:165–185, 2003.

https://doi.org/10.4208/cicp.040913.220115a Published online by Cambridge University Press

[18] M. Junk and W.-A. Yong. Weighted ℓ^2-stability of the lattice Boltzmann method. *SIAM Journal on Numerical Analysis*, 47:1651–1665, 2009.
[19] J.M.V.A. Koelman. A simple lattice Boltzmann scheme for Navier-Stokes fluid flow. *Europhysics Letters*, 15:603–607, 1991.
[20] P. Lallemand and L.-S. Luo. Theory of the lattice Boltzmann method: Dispersion, dissipation, isotropy, Galiean invariance, and stability. *Physical Review E*, 61:6546–6562, 2000.
[21] P. Lallemand and L.-S. Luo. Theory of the lattice Boltzmann method: Acoustic and thermal properties in two and three dimensions. *Physical Review E*, 68:036706, 2003.
[22] L.-S. Luo. Unified theory of lattice Boltzmann models for nonideal gases. *Physical Review Letters*, 81:1618–1621, 1998.
[23] R.W. Mei, L.-S. Luo, P. Lallemand, and D. d'Humières. Consistent initial conditions for lattice Boltzmann simulations. *Computers & Fluids*, 35:855–862, 2006.
[24] C.X. Pan, L.-S. Luo, and C.T. Miller. An evaluation of lattice Boltzmann schemes for porous medium flow simulation. *Computers & Fluids*, 35:898–909, 2006.
[25] Y.H. Qian. Simulating thermohydrodynamics with lattice BGK models. *Journal of Scientific Computing*, 8:231–242, 1993.
[26] Y.H. Qian, D. d'Humières, and P. Lallemand. Lattice BGK models for Navier-Stokes equation. *Europhysics Letters*, 17:479–484, 1992.
[27] Y.H. Qian, S. Succi, and S.A. Orszag. Recent advances in lattice Boltzmann computing. *Annual Reviews Of Computational Physics*, 3:195–242, 1995.
[28] X.W. Shan and H.D. Chen. Lattice Boltzmann model for simulating flows with multiple phases and components. *Physical Review E*, 47:1815–1819, 1993.
[29] P.A. Skordos. Initial and boundary conditions for the lattice Boltzmann method. *Physical Review E*, 48:4823–4842, 1993.
[30] Y. Sone. *Kinetic Theory and Fluid Dynamics*. Birkhäuser, 2002.
[31] P. Van Leemput, M. Rheinläder, and M. Junk. Smooth initialization of lattice Boltzmann schemes. *Computers and Mathematics with Applications*, 58:867–882, 2009.
[32] W.-A. Yong and L.-S. Luo. Nonexistence of H theorems for the athermal lattice Boltzmann models with polynomial equilibria. *Physical Review E*, 67:051105, 2003.
[33] W.-A. Yong and L.-S. Luo. Nonexistence of H theorem for some lattice Boltzmann models. *Journal of Statistical Physics*, 121:91–103, 2005.
[34] W.-A. Yong and L.-S. Luo. Accuracy of the lattice Boltzmann method for the stress. *Physical Review E*, 86:5701, 2012.
[35] H.D Yu, S.S. Girimaji, and L.-S. Luo. Lattice Boltzmann simulations of decaying homogeneous isotropic turbulence. *Physical Review E*, 71:016708, 2005.

https://doi.org/10.4208/cicp.040913.220115a Published online by Cambridge University Press